



**Correlated two-leviton states in the fractional quantum Hall regime**Bruno Bertin-Johannet,<sup>1,\*</sup> Alexandre Popoff ,<sup>1,2</sup> Flavio Ronetti,<sup>1</sup> Jérôme Rech,<sup>1</sup> Thibaut Jonckheere,<sup>1</sup> Laurent Raymond ,<sup>1</sup> Benoit Grémaud,<sup>1</sup> and Thierry Martin<sup>1</sup><sup>1</sup>*Aix Marseille Univ, Université de Toulon, CNRS, CPT, 13009 Marseille, France*<sup>2</sup>*Collège de Tipaerui, BP 4557-98713 Papeete, Tahiti, French Polynesia*

(Received 3 August 2023; accepted 8 December 2023; published 30 January 2024)

We consider a two-dimensional electron system in the Laughlin sequence of the fractional quantum Hall regime to investigate the effect of strong correlations on the mutual interaction between two levitons, single-electron excitations generated by trains of quantized Lorentzian pulses. We focus on two-leviton states injected in a single period with a time separation  $\Delta t$ . In the presence of a quantum point contact operating in the weak-backscattering regime, we compute the backscattered charge by means of the Keldysh technique. In the limit of an infinite period and zero temperature, we show that the backscattered charge for a two-leviton state is not equal to twice the backscattered charge for a single leviton. We present an interpretation for this result in terms of the wave-packet formalism for levitons, thus proposing that an effective interaction between the two levitons is induced by the strongly correlated background. Finally, we perform numerical calculations in the periodic case by using the Floquet formalism for photoassisted transport. By varying the system parameters such as pulse width, filling factor, and temperature we show that the value of the backscattered charge for two-leviton states is strongly dependent on the pulse separation, thus opening scenarios where the effective interaction between levitons can be controllably tuned.

DOI: [10.1103/PhysRevB.109.035436](https://doi.org/10.1103/PhysRevB.109.035436)**I. INTRODUCTION**

The manipulation of individual quantum systems is at the heart of current research in physics aiming at fostering the development of new applications in the domain of quantum technologies [1–3]. Historically, the principal effort has been devoted to the generation and control of photons, the quanta of light, leading to the proposal of quantum computation schemes based on single-photon states [4–8]. Recently, a fast progress in nanoelectronics paved the way towards the manipulation of single-electron states [9–15]. This great interest in the generation and control of single-electron states has led to the development of a new research field which has been called electron quantum optics (EQO) [16–19].

The major step at the foundations of EQO has been the experimental realization of single-electron sources [12]. The first proposal to inject a single electron into the filled Fermi sea of a mesoscopic channel was introduced by Büttiker and collaborators and is known as the mesoscopic capacitor [20,21]. In their proposal, the energy levels of a quantum dot are periodically driven leading to the alternate emission of an electron and a hole into a two-dimensional electron system [22,23]. Despite the fact that this source has been actually realized in experiments [24,25], it requires complex nanolithography techniques to properly design quantum dots. Moreover, despite some theoretical proposals [26], it is also difficult to generalize this experimental protocol to the emission of multiple electronic excitations in the same period.

Both issues can be overcome by considering a different injection scheme based on a time-dependent drive [27,28]. As shown by Levitov and coworkers [29], a train of quantized Lorentzian voltage pulses injects single- and few-electron states, namely, propagating wave packets carrying a single electron devoid of additional particle-hole pairs [30–33], into ballistic quantum channels. These minimal excitations have been called levitons and they have been proved to induce the minimal excess current noise when injected into ballistic channels of mesoscale devices. Due to the intrinsic property of this source,  $q$  different levitons can be injected in a single period and travel unhindered along ballistic channels. The many-body states that are consequently formed are called multielectron levitons or, simply,  $q$  levitons [34–36].

The tools of quantum transport have been widely employed in the context of EQO to investigate the properties of these excitations propagating in ballistic edge channels [37,38]. In particular, the electrical shot noise [39], induced by the granularity of electrons, has proven to be an invaluable source of information to probe the discrete nature of propagating single-electron states. Ground-breaking experimental results have opened the way to the triggered emission and manipulation of single-electron excitations by adapting quantum optics results to the realm of condensed matter. In the first phase of EQO these experiments have shown that it is possible to reproduce the phenomenology of standard quantum optics in mesoscopic fermionic systems in the absence of interaction between electrons [17,40–42], by replacing the bosonic statistics of photons with the Fermi-Dirac statistics. Interestingly, compared to photons, electrons can interact with each other and with the electromagnetic background, thus

\*bruno.bertin@etu.univ-amu.fr

rendering extremely appealing to investigate the effects of the electron-electron interaction on single-electron states. Indeed, a great interest has been devoted to the study of the effects of different types of solid-state correlations on the propagation of levitons, for instance, in systems with superconductivity [43–45] or Coulomb interaction [46–52].

The fractional quantum Hall effect (FQHE) represents a seminal example of strongly correlated states where the interaction between electrons cannot be neglected [53,54]. In the Laughlin sequence of the FQHE a single chiral channel exists at the boundary of the system and the excitations are exotic quasiparticles with fractional charge and statistics called anyons [55–58]. The propagation of levitons in these exotic states of matter is currently under investigation. Importantly, it has been shown that quantized Lorentzian pulses still inject minimal single-electron excitations even in fractional quantum Hall channels [59]. Intriguingly, the propagation of levitons in these edge states has proven to lead to nontrivial properties, which have no counterparts for noninteracting systems [35]. Indeed, in the case of multilevitons, the strongly correlated background rearranges the charge density into an oscillating pattern after a tunneling at the quantum point contact (QPC), leading to the so-called crystallization of levitons, in analogy with the formation of Wigner crystals in one-dimensional systems [60–62]. These works prove that the injection of levitons in a fractional quantum Hall bar still presents many nontrivial aspects to investigate.

Recently, in the context of EQO, the idea of implementing quantum information and computation schemes based on the concept of electron flying qubit has attracted a lot of attention [11,12,15,63–67]. In analogy with previous proposals for photonic states, the qubit states are defined by the presence or the absence of an electron in two alternative propagation paths, which are termed quantum rails. Even in the absence of electron-electron interaction, single-qubit gates can be realized by extended tunneling regions coupling two or more quantum rails in the presence of voltage gates [12,15]. The angle of rotation on the Bloch sphere is proportional to the length of the tunneling region and the voltage applied to the gates, thus allowing for a full control on the single-qubit operation. In contrast, the presence of an interaction between electron flying qubits is a crucial ingredient towards the realization of two-qubit quantum gates and, therefore, universal quantum computation schemes in coherent semiconducting nanoelectronics systems [15,68]. The Coulomb interaction introduces a quantum phase between the two states which is at the origin of the entanglement required to implement a two-qubit gate. However, so far no theoretical proposal or experimental evidence has ever revealed the interaction between two propagating levitons.

In this paper, we intend to elucidate this matter and propose a way to measure the effect of an induced interaction between levitons. Our main emphasis is on the detection of the effect of this interaction between levitons and not on the proposal of quantum information schemes based on the aforementioned interaction. For this purpose, we employ a two-dimensional electron system tuned into the Laughlin sequence of the FQHE in a four-terminal configuration to measure charge-transport properties. We focus on periodic trains of two-leviton states separated by a delay  $\Delta t$ , i.e., we

set the parameter of the Lorentzian voltage so as to inject two levitons per period. As proven in Ref. [69], multiple levitons are still minimal electronic excitations even in the presence of a finite-time delay. By considering a QPC operating in the weak-backscattering regime, we compute the backscattered charge as a function of the separation time between levitons. We first focus on the limit of a single pulse (i.e., infinite period), thus showing that the backscattered charge for a two-leviton state, namely  $Q_2$ , is not equal to twice the backscattered charge  $Q_1$  for a single leviton. We rederive the same result by resorting to the wave-packet formalism for levitons, showing that  $Q_2$  contains a term with four leviton wave functions, in contrast to  $Q_1$  which is expressed in terms of an overlap of only two wave functions. We interpret this additional term in  $Q_2$  as a result of an effective interaction between the two levitons induced by the strongly correlated background. Then, we consider the periodic case and we perform a numerical calculation to show that  $Q_2$  differs from twice  $Q_1$  even for a finite period. Indeed, we show that the time delay  $\Delta t$  between the two pulses can be exploited to reduce, remove, or increase the interaction between levitons in the periodic case. Finally, we address the case of the separated injection of a leviton and an antilevito and show that the backscattered charge is independent of the time delay. We conjecture that our results are valid in any type of Luttinger liquid, including for instance the integer quantum Hall effect at  $\nu = 2$ . The choice of focusing on the Laughlin sequence is motivated by the absence of decoherence induced by other propagating channels [70–72].

The paper is organized as follows. In Sec. II, we introduce the model of the quantum Hall bar with quantum point contact and the source of levitons. In Sec. III, we compute the backscattered charge at the quantum point contact for isolated pulses of levitons and for a periodic drive: we interpret our results by using the wave-packet formalism for levitons. In Sec. IV, we discuss our results by plotting the backscattered charge as a function of different system parameters. In Sec. V, we draw our conclusions.

## II. MODEL

We consider a two-dimensional electron gas in the presence of a strong magnetic field that tunes the system into the FQH regime at filling factor  $\nu = 1/(2n + 1)$ , with  $n \in \mathbb{N}$ , which defines the so-called Laughlin sequence. At filling factors  $\nu < 1$  only the first Landau level is partially filled. In this phase, the bulk is incompressible and insulating from the point of view of quantum transport. The excitations of this incompressible Hall fluid are Laughlin quasiparticles with charge  $e^* = e/3$ . At the boundary of the sample, a gapless chiral edge mode emerges (see Fig. 1). When reservoirs are connected to the system, charge transport occurs from left to right on the top edge and from right to left on the bottom edge, as shown in Fig. 1. This allows us to describe transport properties in terms of two counterpropagating modes existing on two opposite edges of the bar. These modes are connected by a QPC. The latter operates in the weak-backscattering regime, where the tunneling is dominated by Laughlin quasiparticles with charge  $e^* = \nu e$  [73]. A time-dependent voltage  $V(t)$  is applied to terminal  $S$  and the charge backscattered at the QPC is

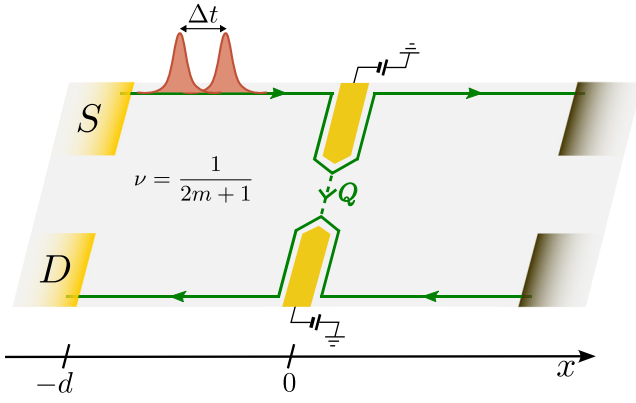


FIG. 1. Schematic view of the setup. A two-dimensional electron system is in the Laughlin series of the FQHE, with a single edge state propagating on the boundary. The system is connected to four terminals: a periodic voltage drive applied to the source terminal  $S$  is injecting multiple levitons in each period separated by a time delay  $\Delta t$  smaller than the period itself. The opposite edges are connected by a QPC placed in  $x = 0$ . The charge backscattered at the QPC, namely  $Q$ , is measured in the drain  $D$ . The remaining terminals (in gray) are grounded and they are not involved in any measurement.

measured in the drain  $D$ . The two remaining terminals are assumed to be grounded. The total Hamiltonian that describes this system is given by  $H = H_0 + H_s + H_B$  and consists of edge states, time-dependent drive, and tunneling terms, respectively.

According to the seminal paper by Wen in Ref. [74], the edge states for the Laughlin sequence can be described in terms of an effective free-boson theory, termed chiral Luttinger liquid. The effective Hamiltonian for the edge states reads as ( $\hbar = 1$ )

$$H_0 = \sum_{r=R,L} \frac{v}{4\pi} \int dx [\partial_x \Phi_r(x)]^2. \quad (1)$$

The right- and left-moving excitations chirally propagating along the two edges are described in terms of bosonic fields  $\Phi_{R/L}$ , satisfying  $[\Phi_{R/L}(x), \Phi_{R/L}(x')] = \pm i\pi \text{sign}(x - x')$  and  $v$  is their velocity. The charge density is defined in terms of bosonic fields as

$$\rho_{R/L}(x) = \pm \frac{e\sqrt{v}}{2\pi} \partial_x \Phi_{R/L}(x). \quad (2)$$

The source of levitons is modeled as a time-dependent drive capacitively coupled to the right-mover edge state by means of a semi-infinite voltage gate. The latter is expressed as  $V_g(x, t) = V(t)\Theta(-x - d)$ , where the Heaviside step function models the semi-infinite contact that ends in  $x = -d$ . The capacitive coupling of this gate to the density of right-moving excitations is described by

$$H_s = \int dx V_g(x, t) \rho_R(x) = V(t) \int dx \Theta(-x - d) \rho_R(x). \quad (3)$$

Equations of motion for the bosonic field  $\Phi_R$  in the presence of the source term are solved in terms of the single-variable fields  $\phi_R$  in the equilibrium configuration  $V(t) = 0$ , thus

giving (see, for instance, Ref. [69])

$$\Phi_R\left(t - \frac{x}{v}\right) = \phi_R\left(t - \frac{x}{v}\right) - \frac{1}{\sqrt{v}} \varphi\left(t - \frac{x}{v}\right), \quad (4)$$

where  $\varphi(t)$  is the phase difference between the two electrodes and is defined as

$$\varphi(t) = e^* \int_{-\infty}^t dt' V(t'). \quad (5)$$

The propagation of bosonic excitations along the edge states remains chiral even in the presence of the driving voltage: this is a consequence of the linear dispersion of edge states for all filling factors in the Laughlin sequence. The profile of these excitations is determined by the time dependence of the phase difference  $\varphi(t)$ . Therefore, the choice of the driving potential is crucial to define the nature of the propagating modes. Here, we focus on periodic trains of Lorentzian-shaped voltage pulses. We consider quantized pulses carrying an integer charge  $-qe = \frac{e^2 v}{2\pi} \int_0^{\mathcal{T}} dt V(t)$ , where  $q$  is any integer number, here named  $q$  levitons. In order to study the effect of the background correlations on  $q$  levitons we take into account the possibility of injecting multiple levitons in one period separated by a delay  $\Delta t$ . The corresponding time-dependent potential is

$$V(t) = \sum_{j=0}^{q-1} \sum_{k=-\infty}^{+\infty} \frac{V_0}{\pi} \frac{\gamma^2}{\gamma^2 + (t - k\mathcal{T} - j\Delta t)^2}, \quad (6)$$

with period  $\mathcal{T} = \frac{2\pi}{\omega}$ , amplitude  $V_0$ , and width at half-height  $2\gamma$ . Later, we will consider also the case of an isolated pulse, which can be recovered from the above expression in the limit  $\gamma \ll \mathcal{T}$ . In Fig. 2, we present some examples for this voltage drive, both for the single-pulse (top panel) and the periodic (bottom panel) cases. Except for very narrow pulses, pulses in different periods always overlap and the signal cannot fully vanish. This is a distinctive difference between isolated pulses and periodic case.

Finally, we consider the tunneling between the two edges which occurs through a QPC at  $x = 0$ . For this reason we can set  $x = 0$  in Eq. (4) and consider only the time dependence of fields. Assuming that the QPC is working in the weak-backscattering regime, the tunneling of Laughlin quasiparticles between opposite edges is the only relevant process [75–77]. Annihilation fields for Laughlin quasiparticles carrying fractional charge  $-ve$  (with  $e > 0$ ) are defined through the standard procedure of bosonization [74]. They read as

$$\Psi_{R/L}(t) = \frac{\mathcal{F}_{R/L}}{\sqrt{2\pi a}} e^{-i\sqrt{v}\Phi_{R/L}(t)} = e^{i\varphi(t)} \psi_{R/L}(t), \quad (7)$$

where  $a$  is a short-distance cutoff and  $\mathcal{F}_{R/L}$  are the Klein factors [39,74,78,79] and we introduced the fermionic fields at equilibrium ( $V = 0$ )

$$\psi_{R/L}(t) = \frac{\mathcal{F}_{R/L}}{\sqrt{2\pi a}} e^{-i\sqrt{v}\phi_{R/L}(t)}. \quad (8)$$

The backscattered Hamiltonian reads as

$$H_B = \lambda \sum_{\epsilon=+,-} [\Psi_R^\dagger(t) \Psi_L(t)]^\epsilon, \quad (9)$$

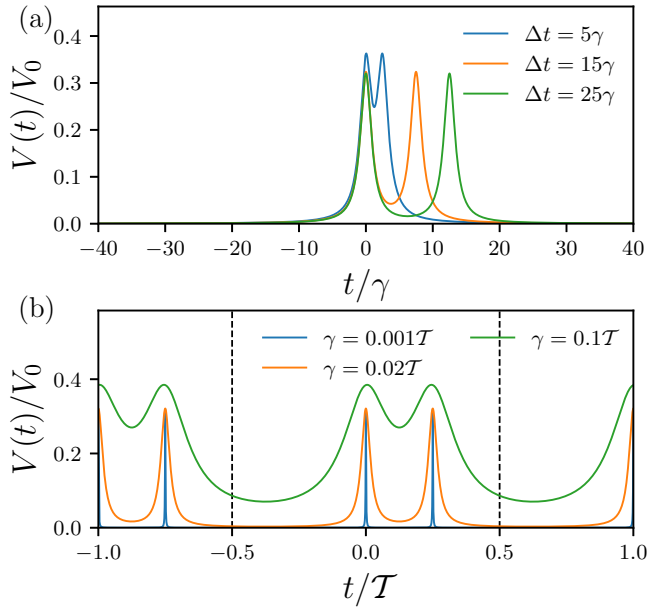


FIG. 2. Time-dependent voltage drive. (a) Case of isolated Lorentzian pulses separated for different values of the time delay  $\Delta t$ . Far before and far after the pulses, the signal is strictly vanishing. (b) Case of a periodic train of Lorentzian pulses for different values of the width  $\gamma$ .

$\lambda$  is the amplitude of tunneling at the QPC and  $\epsilon = -$  means Hermitian conjugate. By expressing the Hamiltonian in terms of fields at equilibrium, we obtain

$$H_B = \lambda \sum_{\epsilon=+,-} [e^{-i\varphi(t)} \psi_R^\dagger(t) \psi_L(t)]^\epsilon. \quad (10)$$

### III. CHARGE BACKSCATTERED AT THE QPC

We are interested in investigating the properties of the charge backscattered at the QPC. Indeed, the transport properties before the QPC do not carry any information about the effect of strong correlations of the propagation of  $q$  levitons, as shown in Ref. [35]. Nevertheless, we expect that, due to the nonlinear nature of the tunneling at the QPC, effects of interaction will be manifested in the backscattered charge. For a periodic time-dependent voltage, the charge which is backscattered in one period  $\mathcal{T}$  is given by

$$Q = \int_{-\mathcal{T}/2}^{\mathcal{T}/2} dt \langle I_B(t) \rangle, \quad (11)$$

where we introduce the backscattering current

$$I_B(t) = ie^* \lambda \sum_{\epsilon=+,-} \epsilon [e^{i\varphi(t)} \psi_R(t)^\dagger \psi_L(t)]^\epsilon. \quad (12)$$

The assumption of weak-backscattering regime allows us to calculate the excess charge density perturbatively in the

tunneling Hamiltonian  $H_B$ . Thermal averages are thus performed over the initial equilibrium density matrix in the absence of tunneling. In order to properly manage the out-of-equilibrium dynamics of the system, calculations are usefully carried out in the Keldysh formalism. To lowest order in the tunneling amplitude  $\lambda$ , the backscattered charge becomes

$$Q = i \frac{e^* \lambda^2}{2\pi^2 a^2} \int_{-\infty}^{+\infty} d\tau e^{2v\mathcal{G}(\tau)} \int_{-\mathcal{T}/2}^{\mathcal{T}/2} dt \sin[\varphi(t) - \varphi(t - \tau)], \quad (13)$$

where we introduced the connected bosonic Green's function  $\mathcal{G}(\tau) = \langle \phi_{R/L}(\tau) \phi_{R/L}(0) \rangle_c$ . Its expression for a finite temperature  $\theta$  reads as ( $k_B = 1$ )

$$\mathcal{G}(\tau) = \log \left[ \frac{\pi \theta \tau}{\sinh(\pi \theta \tau) (1 + i \frac{\tau}{\tau_0})} \right], \quad (14)$$

with  $\tau_0 = a/v$  is the short-time cutoff: our theoretical description is valid for times much longer than  $\tau_0$ .

The expressions for the backscattered charge  $Q$  are valid for any arbitrary driving voltage  $V(t)$ . In the following, we focus specifically on the case of  $q$  levitons, by using the time-dependent potential defined in Eq. (6) for  $q = 1$  and 2. In the latter case, we will assume a time delay  $\Delta t$  between the two levitons. Before numerically evaluating  $Q$  for a finite period  $\mathcal{T}$ , we start by considering the case of isolated pulses ( $\gamma \ll \mathcal{T}$ ) and zero temperature. In this case, we can provide analytical expressions for the backscattered charge that will set the stage for our later discussion.

For the sake of completeness, we will also present the calculations for the charge fluctuations in the case of isolated pulses at zero temperature. This would provide a full characterization of the transport properties of this setup in the presence of one-leviton and two-leviton states.

#### A. Isolated pulses

##### 1. Backscattered charge

In the case of isolated pulses the integral over  $t$  in Eq. (11) can be extended from  $-\infty$  to  $+\infty$  and can be solved analytically. Let us comment that this limit is well defined only for voltage pulses that go to zero at  $t = \pm\infty$ , which is the case for Lorentzian-shaped pulses. The expression for the charge becomes

$$Q = i \frac{e^* \lambda^2}{2\pi^2 a^2} \int_{-\infty}^{+\infty} d\tau e^{2v\mathcal{G}(\tau)} \int_{-\infty}^{+\infty} dt \sin[\varphi(t) - \varphi(t - \tau)]. \quad (15)$$

The integral over  $t$  can be solved analytically for integer values of  $q$ . For  $q = 1$ , one finds

$$Q_1 = \frac{4ie^*}{\pi a^2} \lambda^2 \gamma^2 \int_{-\infty}^{+\infty} d\tau e^{2v\mathcal{G}(\tau)} \frac{\tau}{\tau^2 + 4\gamma^2}. \quad (16)$$

Next, we consider the case  $q = 2$  where the isolated pulses are separated by a constant delay  $\Delta t$ . The integral over  $t$  gives

$$Q_2 = \frac{16ie^*}{\pi a^2} \lambda^2 \gamma^2 \int_{-\infty}^{+\infty} d\tau e^{2v\mathcal{G}(\tau)} \frac{\tau [(4\gamma^2 + \Delta t^2)^2 - \tau^2 (3\Delta t^2 + 4\gamma^2) + 2\tau^4]}{(\tau^2 + 4\gamma^2) [(\Delta t + \tau)^2 + 4\gamma^2] [(\Delta t - \tau)^2 + 4\gamma^2]}. \quad (17)$$

These two expressions can be computed numerically at finite temperature  $\theta$ . Nevertheless, one can obtain an analytical expression for  $Q_1$  and  $Q_2$ . Indeed, by using the zero-temperature limit of the bosonic Green's function

$$G(\tau) = -\log\left(1 + i\frac{\tau}{\tau_0}\right), \quad (18)$$

the residue theorem can be used to calculate the integral over  $t$ , thus arriving to the final expression for the backscattered charge in the case  $q = 1$ ,

$$Q_1 = e^*\left(\frac{\lambda}{v}\right)^2 \left(\frac{2\gamma}{\tau_0}\right)^{2-2\nu} + O\left[\left(\frac{\tau_0}{\gamma}\right)^{2\nu-1}\right], \quad (19)$$

where we kept only the leading order in  $\tau_0/\gamma$ . By performing a similar calculation for  $Q_2$  in the limit of zero temperature, we find at the lowest order in  $\tau_0/\gamma$

$$Q_2 = Q_1 \left\{ 2 \operatorname{Re} \left[ \left(1 + \frac{2i\gamma}{\Delta t}\right)^2 \left(1 - \frac{i\Delta t}{2\gamma}\right)^{-2\nu} \right] + 2 \left(1 + \frac{4\gamma^2}{\Delta t^2}\right) \right\} + O\left[\left(\frac{\tau_0}{\gamma}\right)^{2\nu-1}\right]. \quad (20)$$

We note that, at zero temperature, the backscattered charge for two pulses is proportional to the backscattered charge for a single pulse. For the integer filling factor  $\nu = 1$ , we recover the trivial result that  $Q_2 = 2Q_1$ . Nevertheless, for fractional filling factor, the constant of proportionality depends on  $\Delta t$  and  $\gamma$  and  $Q_2 \neq 2Q_1$ . From this result we can conclude that the charge backscattered when two levitons are impinging at the QPC does not amount in general to twice the charge backscattered when a single leviton is injected. This result is a consequence of the strong correlations that characterize Laughlin states and that introduce a nonlinear current-to-voltage characteristic in the presence of the tunneling of quasiparticles at the QPC.

Before concluding this part, it is instructive to analyze two extreme limits of the ratio  $\Delta t/\gamma$  at zero temperature. In the limit of simultaneous pulses, which can be obtained by setting  $\Delta t/\gamma \ll 1$  in Eq. (20), we find

$$\lim_{\Delta t/\gamma \rightarrow 0} Q_2 = 2Q_1(2 - 3\nu + 2\nu^2). \quad (21)$$

In this limit the constant of proportionality acquires a simple expression, becoming independent of  $\gamma$  and being determined solely by the filling factor  $\nu$ .

Finally, we consider the opposite case of well-separated pulses, which can be found by taking the limit  $\Delta t/\gamma \rightarrow \infty$ . By using the expression  $Q_2$  in Eq. (20), we can compute this limit analytically in the zero-temperature case, thus obtaining

$$\lim_{\Delta t/\gamma \rightarrow \infty} Q_2 = 2Q_1. \quad (22)$$

Indeed, in this case, we recover for any filling factor the trivial result that the charge backscattered for two levitons is twice

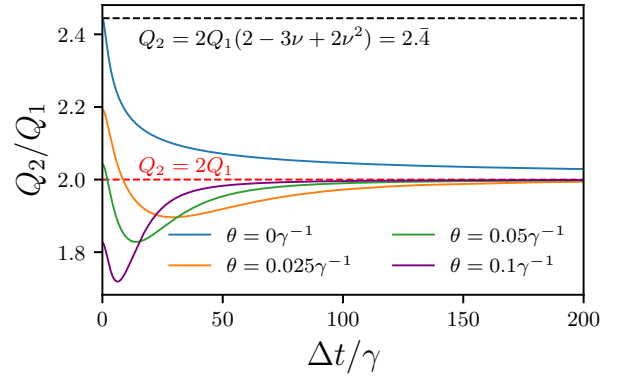


FIG. 3. Backscattered charge for a two-leviton state  $Q_2$  rescaled with respect to the same quantity for a single leviton as a function of  $\Delta t/\gamma$  at different temperatures. The blue line corresponds to the analytical formula at zero temperature and valid in the limit  $\tau_0 \ll \gamma$ . Black and red dotted lines are, respectively, the limits of simultaneous ( $\Delta t/\gamma \rightarrow 0$ ) and well-separated pulses ( $\Delta t/\gamma \rightarrow \infty$ ). The other curves have been computed numerically by fixing  $\tau_0 = 10^{-4}\gamma$ . The only other parameter is the filling factor  $\nu = \frac{1}{3}$ .

the one obtained with a single leviton. For well-separated injection time, the system has relaxed to equilibrium when the second pulse comes in. As a result, the two levitons behave as two independent single pulses. We summarize these results in Fig. 3, where the black and red dotted lines represent the two limits of simultaneous and well-separated pulses at zero temperature.

## 2. Charge fluctuations

In order to further characterize the transport properties of this system, we provide here the analytical calculations of charge fluctuations, which are defined as

$$S_Q = \int_{-\infty}^{+\infty} dt \int_{-\infty}^{+\infty} dt' \langle I_B(t) I_B(t') \rangle - Q^2. \quad (23)$$

Similarly to the backscattered charge, we compute the above integral at zero temperature and for isolated quantized Lorentzian pulses, in order to provide the analytical expressions of charge fluctuations for  $q = 1$  and 2. Before providing the results, we notice that charge fluctuations diverge at zero temperature: as discussed in Ref. [80], the integral should be regularized by subtracting its value at equilibrium, i.e., in the absence of voltage pulses. Therefore, one finds

$$\tilde{S}_Q = \left(\frac{e^*\lambda}{\pi a}\right)^2 \int_{-\infty}^{+\infty} d\tau e^{2\nu G(\tau)} \times \int_{-\infty}^{\infty} dt \{ \cos[\varphi(t) - \varphi(t - \tau)] - 1 \}, \quad (24)$$

where we choose the notation  $\tilde{S}_Q$  for the regularized charge fluctuations. The calculation of the integrals over  $t$  can be performed analytically for integer values of  $q$  using the residue theorem, thus obtaining

$$\tilde{S}_{Q,1} = -e^* \frac{4e^*\lambda^2\gamma}{\pi v_F^2 \tau_0^2} \int_{-\infty}^{+\infty} d\tau \frac{\tau^2}{\tau^2 + 4\gamma^2} e^{2\nu G(\tau)} \quad (25)$$

for  $q = 1$  and

$$\tilde{S}_{Q,2} = -2\pi\gamma \left( \frac{2e^*\lambda}{\pi a} \right)^2 \int_{-\infty}^{\infty} d\tau \tau^2 \frac{32\gamma^4 + (\Delta t^2 - \tau^2)^2 + 4\gamma^2(3\Delta t^2 - \tau^2)}{\Delta t(\tau^2 + 4\gamma^2)[(\Delta t + \tau)^2 + 4\gamma^2][(\Delta t - \tau)^2 + 4\gamma^2]} \left( 1 + i\frac{\tau}{\tau_0} \right)^{-2\nu} \quad (26)$$

for  $q = 2$ . The residue theorem can be used once again to perform both integrals over  $\tau$  and the final expressions for the charge fluctuations for  $q = 1$  and 2 are

$$\tilde{S}_{Q,1} = 2 \left( \frac{2e^*\lambda\gamma}{v\tau_0} \right)^2 \left( 1 + \frac{2\gamma}{\tau_0} \right)^{-2\nu} \quad (27)$$

and

$$\tilde{S}_{Q,2} = 2 \left( \frac{e^*\lambda}{v_F} \right)^2 \left( \frac{2\gamma}{\tau_0} \right)^{2-2\nu} \left[ 2 \left( 1 + \frac{4\gamma^2}{\Delta t^2} \right) + 2 \operatorname{Re} \left( 1 + \frac{2i\gamma}{\Delta t} \right)^2 \left( 1 - \frac{i\Delta t}{2\gamma} \right)^{-2\nu} \right], \quad (28)$$

where we performed the limit  $\tau_0/\gamma \rightarrow 0$ . It is instructive to introduce a Fano factor for the charge as

$$F_Q = \frac{\tilde{S}_{Q,1,2}}{Q_{1,2}}. \quad (29)$$

We notice that  $F_Q = 2e^*$  for  $q = 1$  and also for  $q = 2$  independently of the separation between the levitons. It is important to remark that the above Fano factor has been defined by employing the regularized charge fluctuations in order to yield Fano relations similar to those existing between current and noise in other setups (see, e.g., Refs. [59] and [69]). Due to the proportionality between regularized charge fluctuations and backscattered charge, the plot of  $S_{Q,2}/S_{Q,1}$  as a function of  $\Delta t/\gamma$  has the exact same behavior as the one depicted in Fig. 3 at zero temperature.

### B. Effect of a finite temperature

In Fig. 3 we also present some curves computed numerically at finite temperature for the backscattered charge. Here, we note that in the limit  $\Delta t/\gamma \rightarrow \infty$  the charge  $Q_2$  eventually reaches the value  $2Q_1$  even for finite values of temperature and we checked that this result is independent of the filling factor. Nevertheless, the curves at finite temperature present some interesting features that deserve additional comments. First of all, the limit of simultaneous pulses is not universal as a function of temperature: it reduces its value for increasing temperature and, eventually, it can acquire a value smaller than  $2Q_1$ . Moreover, we note that, as the time delay  $\Delta t$  is varied, the ratio  $Q_2/Q_1$  can become smaller than 2 for certain values of temperature. We ascribe this effect, which is in striking contrast with the zero-temperature isolated-pulse limit, to the additional timescale  $t_\theta = \theta^{-1}$  introduced at finite temperature which acts as a natural cutoff for the edge-state Green's functions. Finally, it is interesting to point out that, when the temperature is increased, the ratio shows a minimum which gets closer and closer to 0, whose position is proportional to the thermal timescale  $t_\theta$ .

Here, we would like to address with more details the change in sign of the excess charge in the presence of a finite temperature. At zero temperature, the ratio  $Q_2/Q_1$  is always greater than 2 and it decays by showing a slow power-law dependence, which is due to the power-law behavior of the Green's functions of the gapless one-dimensional edge modes.

When we turn to the case of a finite temperature, we introduce an additional timescale  $t_\theta$ : in this case the Green's function of the fractional quantum Hall edge states is exponentially suppressed on a scale set by  $t_\theta$ . Let us write the backscattered charge for one and two levitons as

$$Q_1 = i \frac{e^*\lambda^2}{2\pi^2 a^2} \int_{-\infty}^{+\infty} d\tau e^{2\nu\mathcal{G}(\tau)} \Phi_1(\tau), \quad (30)$$

$$Q_2 = i \frac{e^*\lambda^2}{2\pi^2 a^2} \int_{-\infty}^{+\infty} d\tau e^{2\nu\mathcal{G}(\tau)} \Phi_2(\tau), \quad (31)$$

where

$$\Phi_{1,2}(\tau) = \int_{-\infty}^{+\infty} dt \sin[\varphi_{1,2}(t) - \varphi_{1,2}(t - \tau)] \quad (32)$$

is the phase accumulated by the quasiparticles due to the voltage drive integrated over the time  $t$  for a single leviton and for a two-leviton state, respectively. For the following discussion, it is useful to introduce the excess charge  $\Delta Q$  as

$$\Delta Q \equiv Q_2 - 2Q_1, \quad (33)$$

which represents the backscattered charge in excess compared to the trivial case at  $\nu = 1$ . We note that when  $Q_2/Q_1 > 2$  ( $Q_2/Q_1 < 2$ ), the excess charge  $\Delta Q$  is positive (negative). Then for this quantity one has

$$\Delta Q = i \frac{e^*\lambda^2}{2\pi^2 a^2} \int_{-\infty}^{+\infty} d\tau e^{2\nu\mathcal{G}(\tau)} \Delta\Phi(\tau), \quad (34)$$

where we defined  $\Delta\Phi(\tau) = \Phi_2(\tau) - 2\Phi_1(\tau)$ . The latter can be computed analytically as

$$\Delta\Phi(\tau) = \frac{\tau^3}{(4\gamma^2 + \tau^2)} \frac{(\tau^2 - 12\gamma^2 - \Delta t^2)}{[\Delta t^4 - 2\Delta t^2(\tau^2 - 4\gamma^2) + (4\gamma^2 + \tau^2)^2]}. \quad (35)$$

We plot  $\Delta\Phi(\tau)$  in Fig. 4 for different values of  $\Delta t$ , only for  $\tau > 0$  since  $\Delta\Phi(\tau) = -\Delta\Phi(-\tau)$ .

One can see from this plot that this function is changing sign as a function of  $\tau$  and the crossing point is pushed to the right by increasing the value of  $\Delta t$ . Indeed, by its analytical expression one can deduce that the zeros are located in

$$\bar{\tau} = \sqrt{12\gamma^2 + \Delta t^2}. \quad (36)$$

At temperature zero, the Green's function has a power-law decay and  $\Delta\Phi(\tau)$  contributes fully to the final value of the

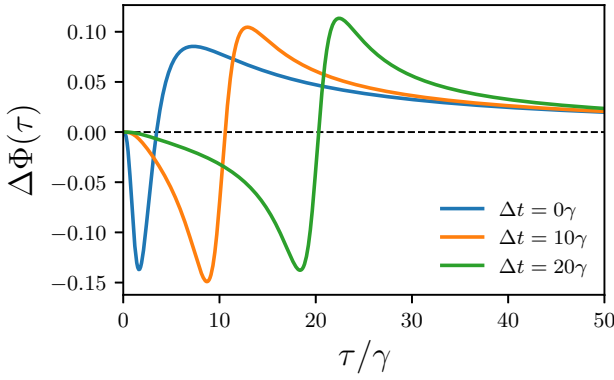


FIG. 4. Excess phase  $\Delta\Phi(\tau) = \Phi_2(\tau) - 2\Phi_1(\tau)$  for different values of the time delay  $\Delta t$  as a function of the time  $\tau$ .

integral over  $\tau$ , such that the long positive tail compensates the initial negative values. In contrast, when we introduce a finite temperature, we expect the positive contribution to be suppressed by the Green's function for certain values of  $\Delta$ . Qualitatively we expect this change in behavior to occur for

$$\overline{\Delta t} \sim \frac{\sqrt{1 - 12\gamma^2\theta^2}}{\pi\theta}. \quad (37)$$

Physically, the above expression corresponds to the time delays at which the effect of temperature starts influencing the excess charge  $\Delta Q$ . In this respect, we can identify three different regimes of temperatures. At zero temperature,  $\overline{\Delta t}$  is diverging, meaning that the effect of temperatures will never appear and, therefore, the ratio  $Q_2/Q_1$  stays always above 2. In the regime of intermediate temperature, one can roughly see that the values given by Eq. (37) are the ones at which the ratio  $Q_2/Q_1$  is crossing the line at  $Q_2/Q_1 = 2$ . Finally, for high enough temperature, the square root becomes imaginary: in this regime  $\overline{\Delta t}$  is not defined. This corresponds to a ratio  $Q_2/Q_1$  which always stays below 2.

$$Q_2 = -\frac{2ie^*}{\pi^2 a^2} \lambda^2 \int_{-\infty}^{\infty} dt \int_{-\infty}^{\infty} d\tau \tau^2 \text{Im}[\chi(t)\chi^*(t-\tau)\chi(t+\Delta t)\chi^*(t-\tau+\Delta t)]e^{2\nu\mathcal{G}(\tau)} + 2Q_1. \quad (41)$$

We note that, while the leviton wave function is strictly valid only for noninteracting systems, the expressions for the backscattered charge are equivalent to the ones obtained in a system without interactions where the Green's functions have been replaced by those of the strongly correlated fractional quantum Hall edge channels. Based on this observation, we claim that we can still use the leviton wave function to support the physical interpretation for our result. A general description of a leviton, even with a fractional charge, in terms of wave functions is possible, but requires a more elaborated formalism [82].

Moreover, we observe that the integral appearing in the above expression is zero for  $\nu = 1$ . Indeed, in this case  $e^{2\mathcal{G}(\tau)}$  is an even function of  $\tau$ , while the imaginary part appearing in Eq. (41) is an odd function of the same variable: therefore, the

In conclusion, we argue that the main reason while at finite temperature the ratio  $Q_2/Q_1$  can go below 2 is due to the presence of an additional timescale, related in this case to  $\theta^{-1}$ . Therefore, we expect to observe a sign switch even for a periodic signal, due to the presence of a finite period  $\mathcal{T}$ . Before showing the numerical results for the periodic case, we present a physical interpretation of the above results in terms of the wave-packet formalism of levitons.

### C. Correlated two-leviton state

In this part, we recast the expression for the backscattered charges  $Q_1$  and  $Q_2$  at zero temperature in terms of the wave function of an isolated leviton. Indeed, a quantized Lorentzian drive with a single peak creates a quantum state of the form [29,81]

$$|\Psi\rangle = \int dx \mathcal{X}^*(x)\psi^\dagger(x)|F\rangle, \quad (38)$$

where  $\psi^\dagger(x)$  creates an electron at the position  $x$ ,  $|F\rangle$  is the ground state of the system, and

$$\mathcal{X}(x-vt) = \sqrt{\frac{\gamma v}{\pi}} \frac{1}{x-vt+iv\gamma} \quad (39)$$

is the wave function of a single leviton propagating in a chiral edge state. By using Eq. (39), the charge  $Q_1$  can be recast as

$$Q_1 = -\frac{e^*\lambda^2}{2\pi^2 a^2} \int_{-\infty}^{\infty} dt \int_{-\infty}^{\infty} d\tau \text{Re}[\chi(t)\chi^*(t-\tau)]\tau e^{2\nu\mathcal{G}(\tau)}, \quad (40)$$

where we defined  $\chi(t) \equiv \mathcal{X}(-vt)$ . We observe that the charge  $Q_1$  contains a product of leviton wave function  $\chi$ , thus showing that it is determined directly by the charge density of the state injected on the system ground state. One can similarly express the charge backscattered by the two-leviton state as

integral over  $\tau$  vanishes at  $\nu = 1$  and one recovers the trivial result  $Q_2 = 2Q_1$  at any temperature.

It is instructive to recast the excess charge  $\Delta Q = Q_2 - 2Q_1$  in terms of the leviton wave function as

$$\Delta Q = \frac{e^*\lambda^2}{4\pi^2 a^2 (i)^{2\nu-2}} \int_{-\infty}^{\infty} dt [\chi(t)g_\nu(t, \Delta t)\chi(t+\Delta t) - \text{H.c.}], \quad (42)$$

where

$$g_\nu(t, \Delta t) = \int_{-\infty}^{\infty} d\tau \chi^*(t-\tau)\chi^*(t-\tau+\Delta t)\tau^2 e^{2\nu\mathcal{G}(\tau)}. \quad (43)$$

In contrast with  $Q_1$ , the excess charge is related to the product of four leviton wave functions, thus proving that it is

originated by a density-density interaction between levitons. We interpret this result by conjecturing that the strongly correlated background mediates an effective interaction between the two levitons.

The function  $g_\nu$  is different from zero for fractional filling factors because of the propagator  $e^{2\nu\mathcal{G}(\tau)}$ . The power-law decay for fractional filling factors is slower than  $\tau^2$ , thus inducing long-time correlations between the two levitons. These correlations do not affect the charge only when the isolated pulses are well separated (limit of  $\Delta t \gg \gamma, 1/\theta$ ). Otherwise, correlations induce an effective interaction between levitons that effectively enhance the value of the charge  $Q_2$  compared to the limit of two well-isolated pulses.

We highlight that the existence of this interaction dramatically relies on the correlations of the FQH background. We base our claim on the fact that for  $\nu = 1$  the interaction between levitons is absent, as discussed below Eq. (41). Indeed, the specific type of this correlation, while influencing the form of the interaction between levitons, is not crucial for its existence. In particular, even at finite temperature, where the power-law behavior of the correlation functions is exponentially suppressed at times  $t > \theta^{-1}$ , the interaction  $g_\nu$  is still present. Since the long-range nature of FQH correlation is not necessary, we will show in the next chapter that our claims are still valid even for a periodic signal, despite the fact that a finite period  $\mathcal{T}$  is cutting the range of correlations. Moreover, we expect the periodic case to be qualitatively similar to the finite-temperature case for isolated pulses and that  $Q_2$  can be smaller than  $2Q_1$ . Nevertheless, for a periodic signal, we expect to recover the limit of well-separated pulses only for very small width  $\gamma$  with respect to the period  $\mathcal{T}$ .

#### D. Periodic train of levitons

In order to make contact with experiments, we consider here the periodic case since the emission of a single isolated pulse is still experimentally challenging. We will show that not only our results still hold, but also that new phenomena emerge. In the case of a periodic signal, no analytical expression can be derived for the backscattered charges  $Q_1$  and  $Q_2$  and one has to resort to a numerical calculation. The latter is conveniently carried out in the photoassisted formalism, where the transport properties are expressed in terms of the Fourier coefficients of the phase associated with the periodic signal [83]. In the following, we will focus only on the case of Lorentzian-shaped pulses with  $q = 1$  and 2.

The photoassisted expressions for the backscattered charges  $Q_1$  and  $Q_2$  are

$$Q_1 = \mathcal{Q} \sum_m p_m^2 \left| \Gamma\left(\nu + i \frac{m+1}{2\theta\pi}\right) \right|^2 \sinh\left(\frac{m+1}{2\theta}\right), \quad (44)$$

$$Q_2 = \mathcal{Q} \sum_m |\tilde{p}_m|^2 \left| \Gamma\left(\nu + i \frac{m+2}{2\theta\pi}\right) \right|^2 \sinh\left(\frac{m+2}{2\theta}\right), \quad (45)$$

where  $\mathcal{Q} = \frac{2e^*}{\mathcal{T}} \left(\frac{\lambda}{v}\right)^2 (2\pi\theta\tau_0)^{2\nu-2} \frac{\theta}{\Gamma(2\nu)}$ . Here, we introduced the photoassisted coefficients for  $q = 1$ ,

$$p_m = \begin{cases} e^{-2\pi\eta m} (1 - e^{-4\pi\eta}), & m \geq 0 \\ -e^{-2\pi\eta}, & m = -1 \\ 0, & m < -1 \end{cases} \quad (46)$$

and for  $q = 2$ ,

$$\tilde{p}_m = \begin{cases} \frac{[1 - e^{i\pi\alpha(m+1)}] - e^{-4\pi\eta - i\pi\alpha} [1 - e^{i\pi\alpha(m+3)}]}{(1 - e^{i\pi\alpha}) e^{i\pi\alpha m}} p_m, & m \geq 0 \\ e^{i\pi\alpha} (e^{-i\pi\alpha} + 1) (1 - e^{-4\pi\eta}) p_{-1}, & m = -1 \\ e^{i\pi\alpha} p_{-1}^2, & m = -2 \\ 0, & m < -2 \end{cases} \quad (47)$$

in terms of the rescaled pulse width  $\eta = \gamma/\mathcal{T}$ , the reduced temperature  $\theta = k_B T/\hbar\omega$ , and the pulse separation  $\alpha = 2\Delta t/\mathcal{T}$ . The sums appearing in Eqs. (44) and (45) can be evaluated numerically: their convergence is ensured by the negative exponential of coefficients  $p_m$  in Eq. (46). As for the case of isolated pulses, we can define an excess charge  $\Delta Q = Q_2 - 2Q_1$  for the periodic drive. We present the corresponding results in the next section by carrying on an analysis over different system parameters. Moreover, we checked that the interpretation of an interaction between levitons induced by the background can be generalized to the periodic case by resorting to the periodic version of leviton's wave functions [34,35].

Concerning the charge fluctuations in the periodic case, in Ref. [69] some of the authors have already shown that a Fano relation exists between noise and backscattered current for one-leviton and multilevton states regardless of the value of the time separation  $\Delta t$ . Therefore, one can conclude that, given the proportionality between charge fluctuations and backscattered charge, the calculation of the latter quantity is sufficient to fully characterize the transport properties of the system. Moreover, it is instructive to point out that the regularized charge fluctuations introduced for isolated pulse in Eq. (24) are the correct expression that is recovered from the periodic case in the limit  $\eta \rightarrow 0$ .

Before concluding this section, we address the case of the injection of two excitations with opposite charge, i.e., one leviton and one antilevton, separated by a time delay  $\Delta t$  in the same period. The form of the applied voltage is

$$V(t) = \sum_{s=\pm} s \sum_{k=-\infty}^{+\infty} \frac{V_0}{\pi} \frac{\gamma^2}{\gamma^2 + (t - k\mathcal{T} + s\Delta t/2)^2}. \quad (48)$$

We note that the voltage is an even function of time, i.e.,  $V(t) = V(-t)$ . By using this property, in Appendix, we show that the backscattered charge induced by this voltage vanishes for any value of  $\Delta t$ . We conclude that for the drive in Eq. (48), the total backscattered charge  $Q_2$  is always identically zero for any choice of system parameters.

The interaction between the leviton and the antilevton cannot be probed by a measure of the backscattered charge. A computation of the charge fluctuations can therefore prove to be useful. To this end, we performed the equivalent of the calculation leading to Eq. (28). This allowed to obtain the charge fluctuations induced by a single couple of leviton and antilevton, which read as

$$\tilde{S}_{Q, \bar{l}l} = 2 \left[ \left( \frac{2\gamma}{\Delta t} \right)^2 + 1 \right]^{-1} \tilde{S}_{Q,l}, \quad (49)$$

where  $l$  stands for leviton and  $\bar{l}$  stands for antilevton. This result can be interpreted as follows: when  $\Delta t/\gamma \rightarrow 0$ , the leviton is superposed with the antilevton in the drive, resulting in



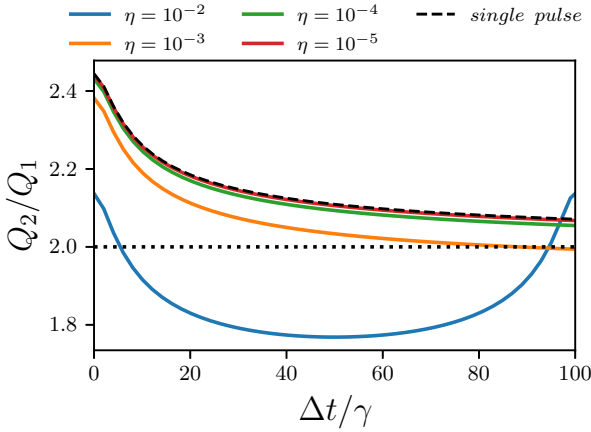


FIG. 5. Backscattered charge for a two-leviton state  $Q_2$  rescaled with respect to the same quantity for a single leviton as a function of  $\Delta t/\gamma$  at zero temperature. The black dashed line is the limit of a single pulse. Solid lines are computed for the periodic case with  $\eta = 10^{-2}, 10^{-3}, 10^{-4}, 10^{-5}$ . We see that for the smallest value of  $\eta = 10^{-5}$ , the periodic case coincides with the analytical limit at infinite period. The black dotted line is a visual guide for  $Q_2 = 2Q_1$ . The ratio  $Q_2/Q_1$  always stays above this line, except for the highest value of  $\eta = 10^{-2}$ : in this case  $Q_2$  can be smaller than twice  $Q_1$ . The only other parameter is the filling factor  $\nu = \frac{1}{3}$ .

no drive at all, and when  $\Delta t/\gamma \rightarrow \infty$  they are well separated and give twice the fluctuations of a single leviton.

Finally, it is worth pointing out that the case of leviton and antilevton is equivalent to an HOM interferometer, where two levitons with the same charge are injected from two opposite terminals, e.g., terminal  $S$  and the gray terminal of left-moving particles in our setup Fig. 1, separated by a controllable time delay. Indeed, we notice that the charge fluctuations for the case of two excitations with opposite charge separated by a time delay correspond to the well-known analytical expression for the charge noise computed in an Hong-Ou-Mandel configuration (see, for instance, Ref. [59]).

#### IV. RESULTS

In the previous section we established a connection between the excess charge  $\Delta Q$  and the effect of the strongly correlated background on the two-leviton state. Here, we discuss our results and present some plots of the latter quantity as a function of different parameters.

##### A. Comparison with the isolated pulse case and effects of time separation

Before investigating the excess charge, in Fig. 5, we plot the backscattered charge  $Q_2$  at filling factor  $\nu = \frac{1}{3}$ , normalized with respect to  $Q_1$ , as a function of  $\Delta t/\gamma$  in the periodic case for different values of the parameter  $\eta = \gamma/\mathcal{T}$ . Here, in order to provide an estimation for the experimentally realistic value of  $\gamma$ , we focus on Lorentzian pulses tailored for future applications in the quantum information domain. In order to couple long enough single-electron excitations in the micrometric tunneling region, short pulses should be realized. It has been estimated that the required pulse width to perform a single-qubit rotation is roughly  $\gamma \sim 10$  ps, which is at the

limit of state-of-the-art technology [15]. Shorter pulses can be envisaged by resorting to schemes based on optoelectronics generation [84]. Since in usual experiments with levitons, the frequency is set to  $\Omega = 2\pi \times 5$  GHz, the resulting value for the renormalized width is  $\eta = 5 \times 10^{-2}$ . While in the following analysis we will consider values of  $\eta$  close to this estimation, in Fig. 5 we consider also smaller values of  $\eta$  in order to compare the charge backscattered with a periodic drive to the same quantity for the case of isolated pulses.

One can clearly see that for  $\eta = 10^{-4}, 10^{-5}$  the colored lines corresponding to the periodic case approach the black dashed line, which corresponds to the case of isolated pulses. This is in agreement with the idea that the case of isolated pulses is recovered in the limit  $\gamma \ll \mathcal{T}$ , as anticipated in the model section. From the analysis of Fig. 5, we can also gather some information concerning a different qualitative behavior of  $Q_2$  with respect to the case of isolated pulses. Indeed, we could check that for  $\eta = 10^{-4}, 10^{-5}$  the ratio  $Q_2/Q_1$  is always greater than or equal to 2: the effect of the correlated background is always to enhance the backscattered charge compared to the case  $\nu = 1$  as for the case of an isolated pulse. Indeed, for  $\eta = 10^{-2}, 10^{-3}$ , we see that the ratio  $Q_2/Q_1$  could be also smaller or equal to 2, thus showing that the effect of the correlated background is strongly affected by the width of Lorentzian pulses in the periodic case. In passing, we comment that this additional feature appears exactly for values of  $\eta$  which are closer to realistic estimation. The effect of a finite period is similar to the one induced by a finite temperature in the sense that it introduces another timescale in the system. Moreover, the overlap between pulses in different periods cannot be avoided, except for very narrow pulses (see the comparison between the single-pulse case and the periodic case with  $\eta = 10^{-5}$  in Fig. 5). As a result, the limit of well-separated pulses is hard to reach in the period case (see Fig. 2).

For this reason, we explore further the dependence of the backscattered charge on parameters  $\alpha = 2\Delta t/\mathcal{T}$  and  $\eta = \gamma/\mathcal{T}$ . In particular, we focus on the quantity  $\Delta Q$  introduced in Eq. (33): for  $\Delta Q > 0$  ( $\Delta Q < 0$ ), the backscattered charge is increased (reduced) by strong correlations with respect to the trivial case at  $\nu = 1$ . In Fig. 6, we present the excess charge as a function of  $\alpha$  for different values of  $\eta$ . Despite the fact that for  $\alpha > 1$  pulses from two neighboring periods are overlapping, we decided to always plot the full interval  $0 < \alpha < 2$ , in order to show the correct periodicity of the backscattered charge. One can deduce from this plot that, for a large range of  $\eta$ , the sign of  $\Delta Q$  can be changed by tuning the parameter  $\alpha$ . Interestingly, there exist some values of  $\alpha$  where the excess charge  $\Delta Q$  vanishes, thus showing that the effect of strong correlations on two-leviton states can be tuned on and off by acting on the separation time  $\Delta t$ . Above a certain value of  $\eta$ , we found that the sign of  $\Delta Q$  is negative for any value of  $\alpha$  at zero temperature and  $\nu = \frac{1}{3}$ . While the specific values of  $\eta$  depend on temperature and filling factor, the important result is that there always exists a width of Lorentzian pulse above which the sign of  $\Delta Q$  is strictly negative.

##### B. Effects of the pulse width

Similarly, in Fig. 7 we explore the behavior of the excess charge as a function of  $\eta$ . In particular, we observe that for

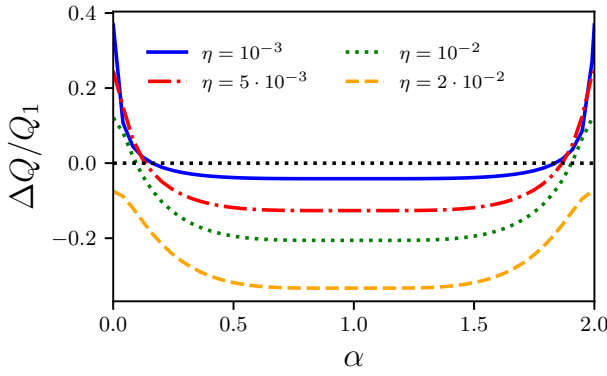


FIG. 6. Excess backscattered charge  $\Delta Q$  rescaled with respect to the backscattered charge  $Q_1$  for a single leviton as a function of  $\alpha = 2\Delta t/\mathcal{T}$  at zero temperature. The black dotted line is a visual guide for  $\Delta Q = 0$ . Solid lines are computed for the periodic case with  $\eta = 10^{-3}, 5 \times 10^{-3}, 10^{-2}, 2 \times 10^{-2}$ . The excess charge  $\Delta Q$  changes sign as a function of  $\alpha$ , except for the highest value of  $\eta = 2 \times 10^{-2}$ : in this case  $\Delta Q$  is always negative. The smaller the value of  $\eta$  and the higher the value of  $\alpha$  at which  $\Delta Q = 0$ . The only other parameter is the filling factor  $\nu = \frac{1}{3}$ .

increasing values of  $\eta$  all the lines reach the asymptotic excess charge  $\Delta Q = Q_1(2^{2\nu-1} - 2)$ , which corresponds to the limit of a constant voltage  $V_{DC} = \hbar\Omega q/e$ . This is in agreement with the fact that the case  $\eta \rightarrow \infty$  corresponds to a constant signal. In the inset of this figure, we zoom in on these curves in the range  $\eta = 10^{-3} - 10^{-2}$ . Again, we observe that for some values of  $\alpha$  and  $\eta$  the excess charge  $\Delta Q$  vanishes and by tuning these parameters its sign can be reversed.

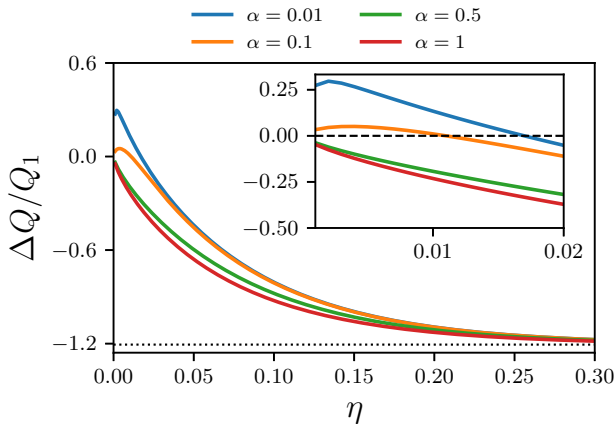


FIG. 7. Excess backscattered charge  $\Delta Q$  rescaled with respect to the backscattered charge  $Q_1$  for a single leviton as a function of  $\eta = \gamma/\mathcal{T}$  at zero temperature. The black dotted line is a visual guide for the limit  $\eta \rightarrow \infty$ : in this case the periodic drive corresponds to a constant voltage with  $q = 2$  and one finds the analytical value of  $\Delta Q = Q_1(2^{2\nu-1} - 2)$ . The other lines are computed for the periodic case with  $\alpha = 0.01, 0.1, 0.5, 1$ . We see that for increasing values of  $\eta$ , all lines tend to the same limit  $\Delta Q = Q_1(2^{2\nu-1} - 2)$ , independently of  $\alpha$ . The only other parameter is the filling factor  $\nu = \frac{1}{3}$ . (Inset) Zoom of the same plot between  $\eta = 0$  and  $\eta = 2 \times 10^{-2}$ : one can see that  $\Delta Q$  changes sign only for  $\alpha = 0.01$  and  $0.1$ .

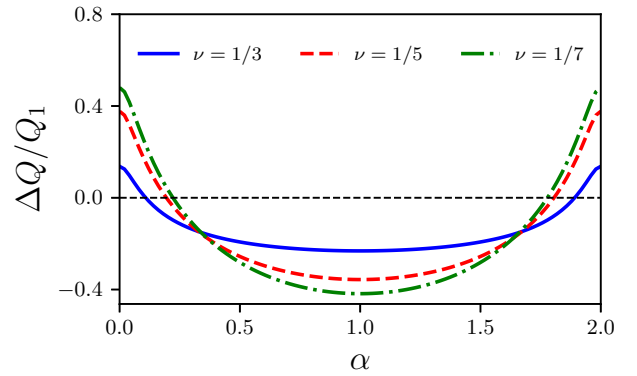


FIG. 8. Excess backscattered charge  $\Delta Q$  rescaled with respect to the backscattered charge  $Q_1$  for a single leviton as a function of  $\alpha = 2\Delta t/\mathcal{T}$  at zero temperature. The black dotted line is a visual guide for  $\Delta Q = 0$  and corresponds to the case  $\nu = 1$ . The other lines are computed for the periodic case with  $\nu = \frac{1}{3}, \frac{1}{5}, \frac{1}{7}$ . The excess charge  $\Delta Q$  is changing sign as a function of  $\alpha$  for all the fractional filling factors. The smaller the value of  $\nu$ , i.e., the stronger the interaction, the higher is the value of  $\alpha$  at which  $\Delta Q$  changes sign. The only other parameter is  $\eta = 10^{-2}$ .

### C. Effects of the filling factor and the temperature

Finally, we discuss the dependence of  $\Delta Q$  from the properties of the strongly correlated background. The latter are encoded in the Green's function which in turn depends on the filling factor  $\nu$  and the temperature  $\theta$ . The dependence of  $\Delta Q$  on the filling factor and, therefore, the strength of the interaction is presented in Fig. 8 for  $\nu = \frac{1}{3}, \frac{1}{5}, \frac{1}{7}$ . In general, we observe two behaviors as the filling factor is reduced. First of all, the values of  $\alpha$  for which the excess charge vanishes increase, thus implying that a stronger interaction requires larger separation time  $\Delta t$  to compensate its effect on the two-leviton state. Moreover, for stronger correlations, the absolute value of the maximum (in  $\alpha = 0$ ) and the minimum (in  $\alpha = 1$ ) of  $\Delta Q$  are also increasing. We study the effect of temperature in Fig. 9. Here, we observe a qualitatively different behavior as a function of  $\alpha$  for different regimes of temperature. For low temperature, the excess charge behaves as the zero-temperature case (blue line): in this case, a single minimum appears at  $\alpha = 1$ . As the temperature is increased, a plateau develops for intermediate values of  $\alpha$ , similarly to the case of isolated pulses presented in Fig. 3. The width of this plateau is roughly proportional to  $\theta^{-1}$ . In the high-temperature limit, two minima appear for values of  $\alpha$  different from  $\alpha = 1$  and whose position scales with the inverse temperature, much like the isolated pulse case of Sec. III A 1. In this regime, the value of  $\Delta Q$  in  $\alpha = 1$  corresponds to a local maximum. In order to make contact with experiments, we comment that for  $\Omega = 2\pi \times 5$  GHz, the temperature  $\theta = \Omega$  corresponds to roughly 1.5 K.

## V. CONCLUSIONS

Here, we considered a quantum Hall bar in the Laughlin sequence of the fractional quantum Hall effect to investigate the effect of a strongly correlated system on the propagation of two-leviton states. These states are injected by periodic

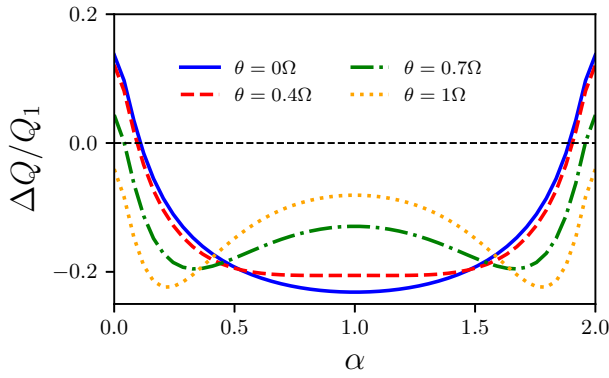


FIG. 9. Excess backscattered charge  $\Delta Q$  rescaled with respect to the backscattered charge  $Q_1$  for a single leviton as a function of  $\alpha = 2\Delta t/T$  for different values of temperature. The black dotted line is a visual guide for  $\Delta Q = 0$ . The other lines are computed for the periodic case with  $\theta = 0, 0.4\Omega, 0.7\Omega, \Omega$ . As the value of temperature is increased, a plateau develops around  $\alpha = 1$ . For higher temperatures, two local minima appear at the left and at the right of  $\alpha = 1$ . The excess charge  $\Delta Q$  is changing sign as a function of  $\alpha$ , except for the highest value of  $\theta = \Omega$ : in this case  $\Delta Q$  is always negative. The other parameters are  $\nu = \frac{1}{3}$  and  $\eta = 10^{-2}$ .

trains of quantized Lorentzian-shaped pulses with width  $\gamma$  and are separated by a controllable  $\Delta t$ . They are minimal electronic excitations, i.e., purely electronic states traveling above the Fermi sea and generating the minimal electrical noise. In the presence of a quantum point contact, we computed the backscattered charge for the low-transparency limit. We presented analytical results in the case of isolated pulses (i.e., infinite period) and zero temperature. We considered the charge backscattered for the two-leviton state, namely  $Q_2$ , and we compared it with the backscattered charge in the presence of a single pulse, termed  $Q_1$ . By an explicit calculation, we showed that  $Q_2 > 2Q_1$  in the fractional regime, in contrast to the trivial result  $Q_2 = 2Q_1$  at  $\nu = 1$ . Interestingly, in the limit of simultaneous pulses ( $\Delta t \ll \gamma$ ), the backscattered charge acquires a simple expression depending only on the filling factor  $\nu$ . By resorting to the wave-packet formalism for levitons, we conjectured the existence of an effective interaction between the two levitons caused by the strongly correlated background. Then, we considered the case of a finite period, performing numerical calculations in the photoassisted formalism. We showed that in the periodic case, as a function of  $\Delta t$ , one can tune the backscattered charge  $Q_2$  to be smaller than, equal to, or greater than  $2Q_1$ . The effects of the correlated background were considered in the dependence of the backscattered charge on the filling factor and on temperature. We based our numerical calculations on realistic

estimations of the parameters that can be realized with state-of-the-art technology. Interesting extension of this work can be the calculation of the backscattered charge in the presence of extended or multiple quantum point contacts, thus taking into account the effect of quantum interference [85–87]. Indeed, the realization of quantum computing architecture with levitons requires the presence of multiple tunneling regions.

## ACKNOWLEDGMENTS

One of us (T.M.) thanks A. Lebedev for early discussions on this topic. This work received support from the French government under the France 2030 investment plan, as part of the Initiative d'Excellence d'Aix-Marseille Université A\*MIDEX. We acknowledge support from the institutes IPhU (Grant No. AMX-19-IET008) and AMUtech (Grant No. AMX-19-IET-01X).

## APPENDIX: LEVITON AND ANTILEVITON CASE

In this Appendix, we compute the charge backscattered at the QPC when terminal 1 is driven by the voltage

$$V(t) = \sum_{s=\pm} s \sum_{k=-\infty}^{+\infty} \frac{V_0}{\pi} \frac{\gamma^2}{\gamma^2 + (t - kT + s\Delta t/2)^2}, \quad (\text{A1})$$

which corresponds to the injection of a leviton and an antileviten in the same period separated by a time delay  $\Delta t$ . In this case,  $V(t) = V(-t)$ . The phase  $\varphi(t)$  becomes in this case

$$\begin{aligned} \varphi(t) &= e^* \int_{-\infty}^t dt' \sum_{s=\pm} s \sum_{k=-\infty}^{+\infty} \frac{V_0}{\pi} \frac{\gamma^2}{\gamma^2 + (t' - kT + s\Delta t/2)^2} \\ &= e^* \int_{t-\Delta/2}^{t+\Delta/2} dt' \sum_{k=-\infty}^{+\infty} \frac{V_0}{\pi} \frac{\gamma^2}{\gamma^2 + (t' - kT)^2}, \end{aligned} \quad (\text{A2})$$

and, as a result,  $\varphi(t) = \varphi(-t)$ . By using the latter property, we show that the integral over  $t$  in Eq. (15) vanishes. Indeed,

$$\begin{aligned} &\int_{-\infty}^{\infty} dt \sin[\varphi(t) - \varphi(t - \tau)] \\ &= \int_{-\infty}^{\infty} dt \sin[\varphi(-t + \tau/2) - \varphi(-t - \tau/2)]. \end{aligned} \quad (\text{A3})$$

By using  $\varphi(t) = -\varphi(-t)$ , we obtain

$$\begin{aligned} &\int_{-\infty}^{\infty} dt \sin[\varphi(t + \tau/2) - \varphi(t - \tau/2)] \\ &= \int_{-\infty}^{\infty} dt \sin[\varphi(t - \tau/2) - \varphi(t + \tau/2)], \end{aligned} \quad (\text{A4})$$

and the integral is obviously zero.

- [1] J. M. Raimond, M. Brune, and S. Haroche, *Rev. Mod. Phys.* **73**, 565 (2001).  
 [2] S. Haroche, *Rev. Mod. Phys.* **85**, 1083 (2013).  
 [3] A. Blais, A. L. Grimsmo, S. M. Girvin, and A. Wallraff, *Rev. Mod. Phys.* **93**, 025005 (2021).

- [4] E. Knill, R. Laflamme, and G. J. Milburn, *Nature (London)* **409**, 46 (2001).  
 [5] P. Kok, W. J. Munro, K. Nemoto, T. C. Ralph, J. P. Dowling, and G. J. Milburn, *Rev. Mod. Phys.* **79**, 135 (2007).

- [6] A. Peruzzo, J. McClean, P. Shadbolt, M.-H. Yung, X.-Q. Zhou, P. J. Love, A. Aspuru-Guzik, and J. L. O'Brien, *Nat. Commun.* **5**, 4213 (2014).
- [7] P. Lodahl, *Quantum Sci. Technol.* **3**, 013001 (2017).
- [8] S. Wehner, D. Elkouss, and R. Hanson, *Science* **362**, eaam9288 (2018).
- [9] M. D. Blumenthal, B. Kaestner, L. Li, S. Giblin, T. J. B. M. Janssen, M. Pepper, D. Anderson, G. Jones, and D. A. Ritchie, *Nat. Phys.* **3**, 343 (2007).
- [10] P. Roulleau, F. Portier, D. C. Glattli, P. Roche, A. Cavanna, G. Faini, U. Gennser, and D. Mailly, *Phys. Rev. Lett.* **100**, 126802 (2008).
- [11] D. C. Glattli and P. S. Roulleau, *Phys. Status Solidi B* **254**, 1600650 (2017).
- [12] C. Bäuerle, D. C. Glattli, T. Meunier, F. Portier, P. Roche, P. Roulleau, S. Takada, and X. Waintal, *Rep. Prog. Phys.* **81**, 056503 (2018).
- [13] G. Roussely, E. Arrighi, G. Georgiou, S. Takada, M. Schalk, M. Urdampilleta, A. Ludwig, A. D. Wieck, P. Armagnat, T. Kloss, X. Waintal, T. Meunier, and C. Bäuerle, *Nat. Commun.* **9**, 2811 (2018).
- [14] H. Duprez, E. Sivre, A. Anthore, A. Aassime, A. Cavanna, A. Ouerghi, U. Gennser, and F. Pierre, *Phys. Rev. X* **9**, 021030 (2019).
- [15] H. Edlbauer, J. Wang, T. Crozes, P. Perrier, S. Ouacel, C. Geffroy, G. Georgiou, E. Chatzikyriakou, A. Lacerda-Santos, X. Waintal, D. C. Glattli, P. Roulleau, J. Nath, M. Kataoka, J. Splettstoesser, M. Acciai, M. C. da Silva Figueira, K. Öztas, A. Trellakis, T. Grange *et al.*, *EPJ Quantum Technol.* **9**, 21 (2022).
- [16] P. Degiovanni, C. Grenier, and G. Fève, *Phys. Rev. B* **80**, 241307(R) (2009).
- [17] E. Bocquillon, F. D. Parmentier, C. Grenier, J.-M. Berroir, P. Degiovanni, D. C. Glattli, B. Plaçais, A. Cavanna, Y. Jin, and G. Fève, *Phys. Rev. Lett.* **108**, 196803 (2012).
- [18] E. Bocquillon, V. Freulon, F. D. Parmentier, J.-M. Berroir, B. Plaçais, C. Wahl, J. Rech, T. Jonckheere, T. Martin, C. Grenier, D. Ferraro, P. Degiovanni, and G. Fève, *Ann. Phys.* **526**, 1 (2014).
- [19] L. Freise, T. Gerster, D. Reifert, T. Weimann, K. Pierz, F. Hohls, and N. Ubbelohde, *Phys. Rev. Lett.* **124**, 127701 (2020).
- [20] M. Büttiker, H. Thomas, and A. Prêtre, *Phys. Lett. A* **180**, 364 (1993).
- [21] M. Büttiker, *J. Phys.: Condens. Matter* **5**, 9361 (1993).
- [22] D. Ferraro, B. Roussel, C. Cabart, E. Thibierge, G. Fève, C. Grenier, and P. Degiovanni, *Phys. Rev. Lett.* **113**, 166403 (2014).
- [23] D. Ferraro, J. Rech, T. Jonckheere, and T. Martin, *Phys. Rev. B* **91**, 205409 (2015).
- [24] J. Gabelli, G. Fève, J.-M. Berroir, B. Plaçais, A. Cavanna, B. Etienne, Y. Jin, and D. C. Glattli, *Science* **313**, 499 (2006).
- [25] G. Fève, A. Mahé, J.-M. Berroir, T. Kontos, B. Plaçais, D. C. Glattli, A. Cavanna, B. Etienne, and Y. Jin, *Science* **316**, 1169 (2007).
- [26] M. Moskalets, J. Kotilahti, P. Buset, and C. Flindt, *Eur. Phys. J.: Spec. Top.* **229**, 647 (2020).
- [27] L. S. Levitov, H. Lee, and G. B. Lesovik, *J. Math. Phys.* **37**, 4845 (1996).
- [28] D. A. Ivanov, H. W. Lee, and L. S. Levitov, *Phys. Rev. B* **56**, 6839 (1997).
- [29] J. Keeling, I. Klich, and L. S. Levitov, *Phys. Rev. Lett.* **97**, 116403 (2006).
- [30] M. Moskalets, *Phys. Rev. B* **91**, 195431 (2015).
- [31] M. Vanević, J. Gabelli, W. Belzig, and B. Reulet, *Phys. Rev. B* **93**, 041416(R) (2016).
- [32] M. Moskalets, *Phys. Rev. Lett.* **117**, 046801 (2016).
- [33] M. Moskalets, *Phys. Rev. B* **98**, 115421 (2018).
- [34] D. C. Glattli and P. Roulleau, *Phys. E (Amsterdam)* **76**, 216 (2016).
- [35] F. Ronetti, L. Vannucci, D. Ferraro, T. Jonckheere, J. Rech, T. Martin, and M. Sassetti, *Phys. Rev. B* **98**, 075401 (2018).
- [36] M. Moskalets, *Phys. Rev. B* **97**, 155411 (2018).
- [37] M. Moskalets, *Phys. Rev. B* **96**, 165423 (2017).
- [38] R. Bisognin, A. Marguerite, B. Roussel, M. Kumar, C. Cabart, C. Chapdelaine, A. Mohammad-Djafari, J. M. Berroir, E. Bocquillon, B. Plaçais, A. Cavanna, U. Gennser, Y. Jin, P. Degiovanni, and G. Fève, *Nat. Commun.* **10**, 3379 (2019).
- [39] T. Martin, in *Nanophysics: Coherence and Transport*, Les Houches, Session LXXXI, edited by H. Bouchiat, Y. Gefen, S. Guéron, G. Montambaux, and J. Dalibard (Elsevier, Amsterdam, 2005), p. 283.
- [40] J. Dubois, T. Jullien, F. Portier, P. Roche, A. Cavanna, Y. Jin, W. Wegscheider, P. Roulleau, and D. C. Glattli, *Nature (London)* **502**, 659 (2013).
- [41] T. Jullien, P. Roulleau, B. Roche, A. Cavanna, Y. Jin, and D. C. Glattli, *Nature (London)* **514**, 603 (2014).
- [42] J. Kotilahti, P. Buset, M. Moskalets, and C. Flindt, *Entropy* **23**, 736 (2021).
- [43] M. Acciai, F. Ronetti, D. Ferraro, J. Rech, T. Jonckheere, M. Sassetti, and T. Martin, *Phys. Rev. B* **100**, 085418 (2019).
- [44] F. Ronetti, M. Carrega, and M. Sassetti, *Phys. Rev. Res.* **2**, 013203 (2020).
- [45] B. Bertin-Johannet, J. Rech, T. Jonckheere, B. Grémaud, L. Raymond, and T. Martin, *Phys. Rev. B* **105**, 115112 (2022).
- [46] M. Acciai, M. Carrega, J. Rech, T. Jonckheere, T. Martin, and M. Sassetti, *Phys. Rev. B* **98**, 035426 (2018).
- [47] D. Ferraro, F. Ronetti, L. Vannucci, M. Acciai, J. Rech, T. Jonckheere, T. Martin, and M. Sassetti, *Eur. Phys. J.: Spec. Top.* **227**, 1345 (2018).
- [48] L. Vannucci, F. Ronetti, D. Ferraro, J. Rech, T. Jonckheere, T. Martin, and M. Sassetti, *J. Phys.: Conf. Ser.* **969**, 012143 (2018).
- [49] F. Ronetti, L. Vannucci, D. Ferraro, T. Jonckheere, J. Rech, T. Martin, and M. Sassetti, *Phys. Rev. B* **99**, 205406 (2019).
- [50] M. Acciai, A. Calzona, M. Carrega, T. Martin, and M. Sassetti, *New J. Phys.* **21**, 103031 (2019).
- [51] G. Rebora, M. Acciai, D. Ferraro, and M. Sassetti, *Phys. Rev. B* **101**, 245310 (2020).
- [52] G. Rebora, D. Ferraro, R. H. Rodriguez, F. D. Parmentier, P. Roche, and M. Sassetti, *Entropy* **23**, 138 (2021).
- [53] D. C. Tsui, H. L. Stormer, and A. C. Gossard, *Phys. Rev. Lett.* **48**, 1559 (1982).
- [54] R. B. Laughlin, *Phys. Rev. Lett.* **50**, 1395 (1983).
- [55] C. Nayak, S. H. Simon, A. Stern, M. Freedman, and S. Das Sarma, *Rev. Mod. Phys.* **80**, 1083 (2008).
- [56] M. Hashisaka, T. Jonckheere, T. Akiho, S. Sasaki, J. Rech, T. Martin, and K. Muraki, *Nat. Commun.* **12**, 2794 (2021).
- [57] T. Jonckheere, J. Rech, B. Grémaud, and T. Martin, *Phys. Rev. Lett.* **130**, 186203 (2023).

- [58] P. Glidic, O. Maillet, C. Piquard, A. Aassime, A. Cavanna, Y. Jin, U. Gennser, A. Anthore, and F. Pierre, *Nat. Commun.* **14**, 514 (2023).
- [59] J. Rech, D. Ferraro, T. Jonckheere, L. Vannucci, M. Sassetti, and T. Martin, *Phys. Rev. Lett.* **118**, 076801 (2017).
- [60] E. Wigner, *Phys. Rev.* **46**, 1002 (1934).
- [61] H. J. Schulz, *Phys. Rev. Lett.* **71**, 1864 (1993).
- [62] V. V. Deshpande, M. Bockrath, L. I. Glazman, and A. Yacoby, *Nature (London)* **464**, 209 (2010).
- [63] R. P. G. McNeil, M. Kataoka, C. J. B. Ford, C. H. W. Barnes, D. Anderson, G. A. C. Jones, I. Farrer, and D. A. Ritchie, *Nature (London)* **477**, 439 (2011).
- [64] M. Yamamoto, S. Takada, C. Bäuerle, K. Watanabe, A. D. Wieck, and S. Tarucha, *Nat. Nanotechnol.* **7**, 247 (2012).
- [65] D. Dasenbrook and C. Flindt, *Phys. Rev. B* **92**, 161412(R) (2015).
- [66] D. Dasenbrook and C. Flindt, *Phys. Rev. Lett.* **117**, 146801 (2016).
- [67] D. Dasenbrook, J. Bowles, J. B. Brask, P. P. Hofer, C. Flindt, and N. Brunner, *New J. Phys.* **18**, 043036 (2016).
- [68] S. Takeda and A. Furusawa, *Phys. Rev. Lett.* **119**, 120504 (2017).
- [69] L. Vannucci, F. Ronetti, J. Rech, D. Ferraro, T. Jonckheere, T. Martin, and M. Sassetti, *Phys. Rev. B* **95**, 245415 (2017).
- [70] E. Bocquillon, V. Freulon, J.-M. Berroir, P. Degiovanni, B. Plaçais, A. Cavanna, Y. Jin, and G. Fève, *Science* **339**, 1054 (2013).
- [71] C. Wahl, J. Rech, T. Jonckheere, and T. Martin, *Phys. Rev. Lett.* **112**, 046802 (2014).
- [72] A. Marguerite, C. Cabart, C. Wahl, B. Roussel, V. Freulon, D. Ferraro, C. Grenier, J.-M. Berroir, B. Plaçais, T. Jonckheere, J. Rech, T. Martin, P. Degiovanni, A. Cavanna, Y. Jin, and G. Fève, *Phys. Rev. B* **94**, 115311 (2016).
- [73] C. L. Kane and M. P. A. Fisher, *Phys. Rev. B* **46**, 15233 (1992).
- [74] X.-G. Wen, *Adv. Phys.* **44**, 405 (1995).
- [75] C. L. Kane and M. P. A. Fisher, *Phys. Rev. Lett.* **72**, 724 (1994).
- [76] L. Saminadayar, D. C. Glatli, Y. Jin, and B. Etienne, *Phys. Rev. Lett.* **79**, 2526 (1997).
- [77] R. de-Picciotto, M. Reznikov, M. Heiblum, V. Umansky, G. Bunin, and D. Mahalu, *Nature (London)* **389**, 162 (1997).
- [78] J. von Delft and H. Schoeller, *Ann. Phys.* **510**, 225 (1998).
- [79] R. Guyon, P. Devillard, T. Martin, and I. Safi, *Phys. Rev. B* **65**, 153304 (2002).
- [80] T. Jonckheere, M. Creux, and T. Martin, *Phys. Rev. B* **72**, 205321 (2005).
- [81] C. Grenier, J. Dubois, T. Jullien, P. Roulleau, D. C. Glatli, and P. Degiovanni, *Phys. Rev. B* **88**, 085302 (2013).
- [82] H. S. Sim (private communication).
- [83] A. Crépieux, P. Devillard, and T. Martin, *Phys. Rev. B* **69**, 205302 (2004).
- [84] B. Heshmat, H. Pahlevaninezhad, Y. Pang, M. Masnadi-Shirazi, R. B. Lewis, T. Tiedje, R. Gordon, and T. E. Darcie, *Nano Lett.* **12**, 6255 (2012).
- [85] D. Chevallier, J. Rech, T. Jonckheere, C. Wahl, and T. Martin, *Phys. Rev. B* **82**, 155318 (2010).
- [86] L. Vannucci, F. Ronetti, G. Dolcetto, M. Carrega, and M. Sassetti, *Phys. Rev. B* **92**, 075446 (2015).
- [87] F. Ronetti, L. Vannucci, G. Dolcetto, M. Carrega, and M. Sassetti, *Phys. Rev. B* **93**, 165414 (2016).